

Analytical formulation for the bend loss in single-ring hollow-core photonic crystal fibers

MICHAEL H. FROSZ,* PAUL ROTH, MEHMET C. GÜNENDI, AND PHILIP ST.J. RUSSELL

Max Planck Institute for the Science of Light, Staudtstr. 2, D-91058 Erlangen, Germany

*Corresponding author: michael.frosz@mpl.mpg.de

Received 3 November 2016; revised 13 January 2017; accepted 19 January 2017; posted 24 January 2017 (Doc. ID 280041); published 23 February 2017

Understanding bend loss in single-ring hollow-core photonic crystal fibers (PCFs) is becoming of increasing importance as the fibers enter practical applications. While purely numerical approaches are useful, there is a need for a simpler analytical formalism that provides physical insight and can be directly used in the design of PCFs with low bend loss. We show theoretically and experimentally that a wavelength-dependent critical bend radius exists below which the bend loss reaches a maximum, and that this can be calculated from the structural parameters of a fiber using a simple analytical formula. This allows straightforward design of single-ring PCFs that are bend-insensitive for specified ranges of bend radius and wavelength. It also can be used to derive an expression for the bend radius that yields optimal higher-order mode suppression for a given fiber structure. © 2017 Chinese Laser Press

OCIS codes: (060.2280) Fiber design and fabrication; (060.2310) Fiber optics; (060.4005) Microstructured fibers; (060.5295) Photonic crystal fibers.

<https://doi.org/10.1364/PRJ.5.000088>

1. INTRODUCTION

Hollow-core photonic crystal fibers (HC-PCFs) permit light to be guided over long distances in vacuum, gases, or liquids [1]. If light is confined by a full 2D photonic bandgap, such fibers offer ultralow losses over a limited bandwidth, for example, a 200 nm wide transmission window at 1550 nm within which the loss is less than 8 dB/km [2–4]. Another type of HC-PCF, investigated in recent years, guides light with higher loss (typically 1 dB/m or less) but over a much broader bandwidth (several hundreds of nanometers). The confinement mechanism in this case is anti-resonant reflection from an azimuthally periodic structure of hollow channels surrounding the core [5]. Examples include kagomé-style PCFs [6] and PCFs with a single ring of capillaries encircling the core [7]. Single-ring PCFs have recently been receiving increasing attention because of their relative simplicity and surprisingly low loss, enhanced recently by the discovery that higher-order modes can be efficiently suppressed when the ratio between the inner diameter d of the cladding capillaries (anti-resonant elements or AREs) and the diameter D of the core (defined as the minimum distance between two diametrically opposite AREs) is close to 0.68 [8]. Earlier experimental studies focused on fibers with d/D much smaller than 0.68 [7,9,10]. As d/D increases, however, the fiber becomes increasingly bend-sensitive. Although it is known that this occurs due to coupling between the core mode and the surrounding capillaries [11–13], no simple analytical

expression has yet been reported that quantifies the bend-sensitivity for a given structure, although such an expression would permit easy optimization of the fiber design. Numerical solutions of Maxwell's equations yield loss values for specified values of bend radius, structure, and wavelength (e.g., [14,15]) but provide only limited physical understanding of the underlying bend loss mechanisms.

Here we derive, based on an intuitive physical picture, a simple analytical expression for a “critical bend radius” R_{cr} , above which bend loss is negligible (note that the physics underlying the appearance of R_{cr} in single-ring PCFs is slightly different from that seen in conventional step-index fibers [16]).

2. THEORY

Bend loss in fibers comes in two main forms. First, the transition bend loss, which occurs as the radius of curvature is gradually reduced, and second the leakage loss of the eigenmode of the constant-curvature fiber [17]. In this paper, we shall concentrate on the second of these.

The analysis starts with an approximate expression for the effective phase index of the LP_{pq} -like mode in a circular glass capillary, first derived by Marcatili and Schmeltzer [18]:

$$n_{pq} = \sqrt{1 - \left(\frac{u_{pq} \lambda}{\pi d_i}\right)^2}, \quad (1)$$

where u_{pq} is the q -th zero of the Bessel function J_p , λ is the wavelength, and d_i is the inner diameter of the capillary $\{D$ for the core and d for the capillaries [see Fig. 1(a)].

When the fiber is bent to the radius of curvature R , the refractive index distribution becomes tilted (to first order) as follows [19]:

$$\hat{n}(x, y) = \left(1 + \frac{y}{R}\right) \bar{n}(x, y), \quad (2)$$

where R is the bend radius, and the (x, y) axes lie in the local transverse fiber plane, the y axis pointing normal to the bend, the fiber axis being located at $y = 0$. The effective index of the LP₀₁ mode of a cladding capillary rotated at angle θ to the y axis [see Fig. 1(a)] is then given by Eq. (2) with $y = [(d + D)/2] \cos \theta$.

The index difference between an LP₀₁ core mode and the LP₀₁ capillary mode takes the analytical form:

$$\Delta n_{01}^{pq} = \sqrt{1 - \left(\frac{u_{pq} \lambda}{\pi D}\right)^2} - \sqrt{1 - \left(\frac{u_{01} \lambda}{\pi d}\right)^2} \left(1 + \frac{d + D}{2R} \cos \theta\right). \quad (3)$$

This equation shows that, as the radius of curvature R falls, a critical value R_{cr}^{pq} is reached when $\Delta n_{01}^{pq} = 0$ for $\theta = 0^\circ$, i.e., when one of the cladding capillaries is at its maximum distance $(d + D)/2$ from the x axis. Under these phase-matched

conditions, light couples strongly from the core mode to the outer capillary mode, where it leaks away rapidly into the surrounding solid glass sheath. If the fiber is carefully aligned so that $\theta = 30^\circ$, the critical bend radius will be a factor $\sqrt{3}/2$ smaller. In a typical laboratory setting, however, θ will vary randomly, so that the upper value of R_{cr}^{pq} is likely to apply. Overall, this means that phase-matching between core and capillary modes can in principle occur for any bend radius $R < R_{cr}^{pq}$. Starting with a straight fiber, therefore, the bend loss will increase rapidly when the critical bend radius is reached, and the transmission will remain small for smaller values of R .

Figure 1(b) plots Eq. (3) for the case when $d/D = 0.696$, $p = 0$, and $q = 1$ (i.e., the LP₀₁ core mode, $u_{01} = 2.405$) for four different values of the scale parameter λ/D . This plot predicts, for example, a critical bend radius of ~ 17 cm for $D = 79 \mu\text{m}$, $d = 55 \mu\text{m}$, and $\lambda = 2.8 \mu\text{m}$.

Using the approximation $\lambda/(\pi D) \ll 1$, Eq. (3) can be manipulated to yield an explicit expression for R_{cr}^{01} :

$$\frac{R_{cr}^{01}}{D} = \frac{D^2}{\lambda^2} \cdot \frac{\pi^2}{u_{01}^2} \frac{(d/D)^2}{1 - d/D} \cos \theta, \quad (4)$$

which shows that, for a given structure, the radius of curvature at which bend loss becomes significant scales with D^3/λ^2 . This functional dependence is similar to that seen in standard step-index fiber, i.e., $R_{cr} \propto \rho^3/\lambda^2$ where ρ is the core radius (see, e.g., [20]). The simple expression in Eq. (4) has the advantage of clearly revealing the dependence of R_{cr}^{01} on the scale parameter D/λ and the shape parameter d/D . (Note that a more complicated analysis, based on similar physical assumptions, has been reported in connection with THz guidance in a single-ring polymer structure [11]).

To verify the analysis, we used finite-element modeling (COMSOL) with perfectly matched layer boundary conditions [21]. Numerically simulated modal field (axial component of the Poynting vector) distributions for the structure mentioned above are plotted in Fig. 2 for three different values of R . At $R = 22$ cm, just above $R_{cr}^{01} = 17$ cm, the outermost capillary mode is only weakly excited, and the loss is ~ 1.2 dB/m. At $R = 17$ cm, the bend loss rises to ~ 21 dB/m, and the outermost capillary lights up brightly. At $R = 8.6$ cm, the capillaries at $\theta = \pm 60^\circ$ become resonant, and the bend loss drops to around 5 dB/m, with little difference between polarization states. Because in a typical experiment a fiber will start out straight and then gradually bend to smaller values of R , most of the bend loss will occur when R has values close to R_{cr}^{01} . If R remains constant along the whole fiber length, the loss can attain quite small values provided the core and capillary modes are phase mismatched, which can occur even when R is small.

The numerically calculated bend loss values are plotted versus normalized bend radius in Fig. 3, together with the critical bend radius calculated from Eq. (4) for $\theta = 0^\circ$. The analytical expression provides a good estimate of the bend radius at which the bend loss significantly increases. For both fibers, the bend loss was of order 10 dB/m at the critical bend radius. There is a small offset between the analytically calculated critical bend radii and the peaks in bend loss found from the numerical calculations, but this is not unexpected given the approximations used in deriving Eq. (4).

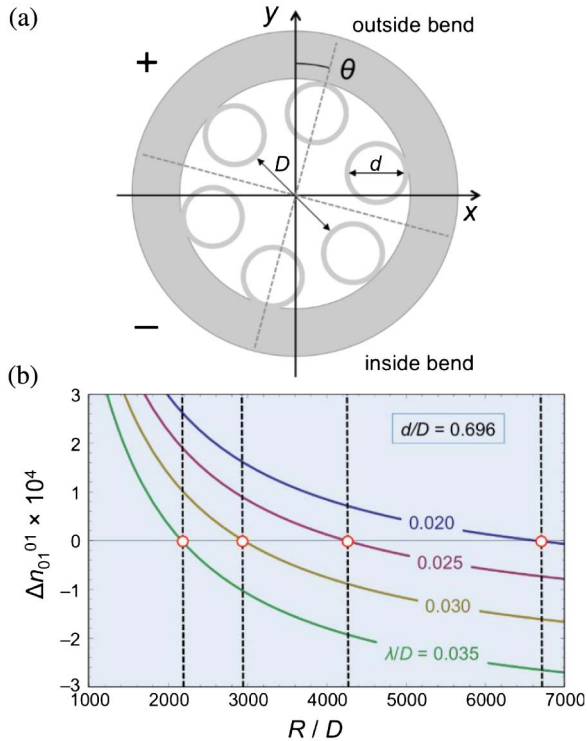


Fig. 1. (a) Sketch of the geometry of a single-ring HC-PCF, showing the local coordinate system. The inner diameter of the six capillaries is d , and the core diameter (the minimum distance between two diametrically opposite capillaries) is D . (b) Index difference Δn_{01}^{01} between LP₀₁-like core and capillary modes, plotted against R/D for $d/D = 0.696$ at four different values of λ/D .

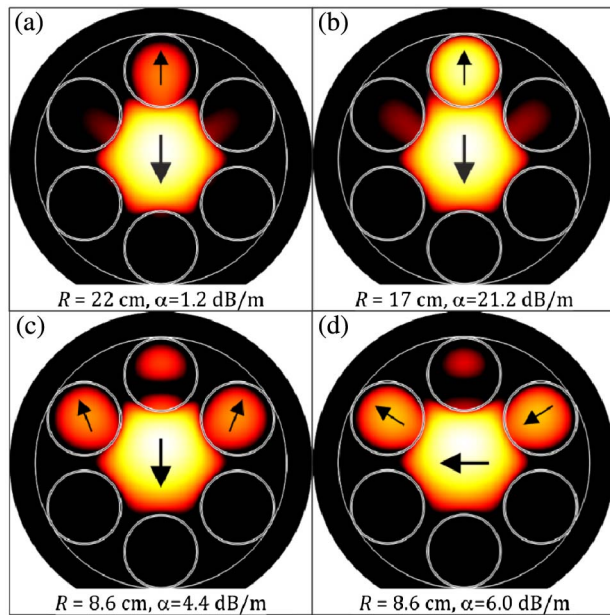


Fig. 2. Numerically calculated axial Poynting vector distributions and loss α of a single-ring PCF with $d = 55 \mu\text{m}$, $D = 79 \mu\text{m}$, $\lambda = 2.8 \mu\text{m}$ and capillary wall thickness $t = 1.15 \mu\text{m}$, for (a) bend radius slightly greater than $R_{\text{cr}}^{01} = 17.2 \text{ cm}$, (b) close to R_{cr}^{01} , and (c) and (d) close to the radius of curvature that phase-matches the LP_{01} core mode to capillaries placed at $\theta = \pm 60^\circ$. The arrows indicate the polarization of the electric field.

3. EXPERIMENTS

To experimentally validate Eq. (4), the bend loss in two different single-ring PCFs was measured by first recording the transmission spectra in few meters lengths of straight fiber. The fibers were then coiled around mandrels of varying radii (in steps of 1.25 cm) without disturbing the in- and out-coupling ends of the fibers, and the transmission spectra measured in each case. Subtracting the transmission spectrum (in dB) of the straight fiber from that of the bent fiber and dividing by the length of bent fiber section gave the bend-induced loss, which is plotted in Fig. 4. The solid white curves in Fig. 4 plot R_{cr}^{01}/D from Eq. (4) for both fibers. It is clear that the bend loss remains relatively low for $R > R_{\text{cr}}^{01}$ but increases rapidly as R_{cr}^{01} is approached, reaching a maximum as R decreases beyond this point. No special care was taken to control the polarization state or the alignment angle θ in Fig. 1(a) because we are only interested in the bend sensitivity of these fibers under normal laboratory conditions. This means that the critical bend radius in some cases will appear at lower values of R , corresponding to $\theta = \pm 30^\circ$, marked by the dashed white lines in Fig. 4. This means that the fiber would in principle be slightly less bend sensitive if carefully oriented at $\theta = \pm 30^\circ$.

The gray-shaded rectangle in Fig. 4(a) marks the wavelength range where there was no measurable transmission even in the straight fiber, which is a consequence of phase-matching to a resonance in the walls of the ring capillaries at wavelengths given by $\lambda_m = 2b(n^2 - 1)^{1/2}/m$, where b is the capillary wall thickness, n is the refractive index of the glass, and m is the order of the resonance [5,22]. For the PCF in Fig. 4(a)

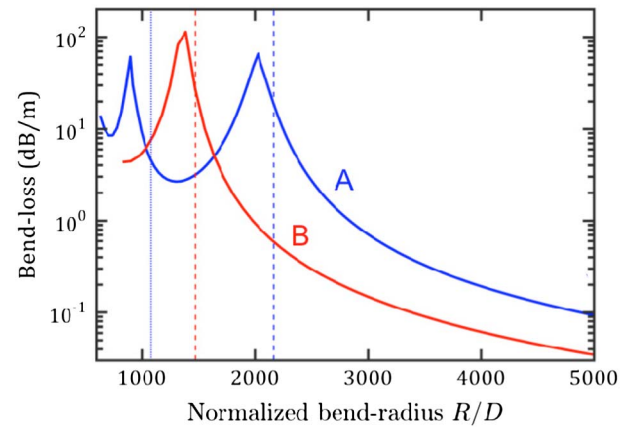


Fig. 3. Numerically calculated bend loss for the fibers for $\theta = 0^\circ$, plotted against normalized bend radius R/D . A: $(d, D, \lambda) = (55, 79, 2.8) \mu\text{m}$, i.e., $d/D = 0.70$ and $\lambda/D = 0.035$. B: $(d, D, \lambda) = (22, 36, 1.2) \mu\text{m}$, i.e., $d/D = 0.61$, $\lambda/D = 0.033$. The dashed vertical lines mark the corresponding analytical solutions for the critical bend radius using Eq. (4) with $\theta = 0^\circ$. The dotted vertical line shows the bend radius for phase-matching to the capillaries at $\theta = \pm 60^\circ$. In each case the loss is calculated for modes polarized normal to the bend, i.e., in the y direction in Fig. 1(a).

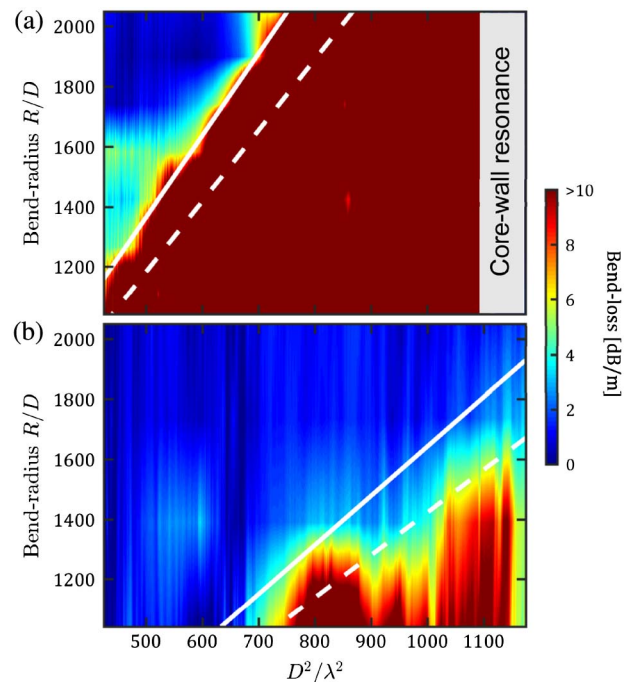


Fig. 4. Experimentally measured bend loss in two fibers with the same shape parameters as in Fig. (3). (a) $d/D = 0.70$ and (b) $d/D = 0.61$. The bend radii were changed in steps of 1.25 cm, and between these steps the colors are interpolated. The measured loss versus wavelength in (b) was smoothed with a moving average filter. The gray rectangle in (a) marks the region where the core mode phase-matches to a resonance in the walls of the capillaries, causing high attenuation. In each case, the white solid and dashed lines are solutions of Eq. (4) for $\theta = 0^\circ$ and $\theta = 30^\circ$, respectively.

$h = 1.15 \mu\text{m}$, yielding $\lambda_1 = 2.36 \mu\text{m}$ ($D^2/\lambda^2 = 1121$). For the PCF in Fig. 4(b) $\lambda \sim 0.97 \mu\text{m}$ ($D^2/\lambda^2 \sim 1377$, $h \sim 0.46 \mu\text{m}$), which lies outside the wavelength range considered. Because in practice a low-loss single-ring PCF will always be used at wavelengths far away from the capillary wall resonances, we do not discuss here how bending might broaden these loss bands.

4. HIGHER-ORDER MODE SUPPRESSION

Moving on now to bend loss for the LP_{11} -like core mode ($u_{11} = 3.832$) and applying the same approximations as used in deriving Eq. (4), we arrive at the result

$$\frac{R_{\text{cr}}^{11}}{D} = \frac{D^2}{\lambda^2} \cdot \frac{\pi^2(1 + d/D)}{(u_{01}D/d)^2 - u_{11}^2} \cos \theta. \quad (5)$$

Under certain conditions, Δn_{01}^{11} can be negative in the straight fiber, which has the interesting consequence that light will leak away toward the *inside* of the bend for bend radii less than R_{cr}^{11} . This occurs when $d/D > u_{01}/u_{11} \approx 0.63$. As previously reported [8], efficient suppression of higher-order core modes in a straight single-ring PCF occurs when $d/D \approx u_{01}/u_{11}$. Equation (5) shows that higher-order core modes can be suppressed in cases when $d/D < 0.63$ by bending to the correct radius of curvature.

5. CONCLUSIONS

The critical bend radius in single-ring HC-PCFs can be accurately predicted using an analytical expression derived from simple physical principles, resulting in values that agree well with experiments. The analysis can also be applied to structures with different numbers of ring capillaries, e.g., eight [13].

REFERENCES

1. P. St.J. Russell, "Photonic-crystal fibers," *J. Lightwave Technol.* **24**, 4729–4749 (2006).
2. P. J. Roberts, F. Couny, H. Sabert, B. J. Mangan, D. P. Williams, L. Farr, M. W. Mason, A. Tomlinson, T. A. Birks, J. C. Knight, and P. St.J. Russell, "Ultimate low loss of hollow-core photonic crystal fibres," *Opt. Express* **13**, 236–244 (2005).
3. M. H. Frosz, J. Nold, T. Weiss, A. Stefani, F. Babic, S. Rammler, and P. St.J. Russell, "Five-ring hollow-core photonic crystal fiber with 1.8 dB/km loss," *Opt. Lett.* **38**, 2215–2217 (2013).
4. Y. Chen, Z. X. Liu, S. R. Sandoghchi, G. T. Jasion, T. D. Bradley, E. N. Fokoua, J. R. Hayes, N. V. Wheeler, D. R. Gray, B. J. Mangan, R. Slavik, F. Poletti, M. N. Petrovich, and D. J. Richardson, "Multi-kilometer long, longitudinally uniform hollow core photonic bandgap fibers for broadband low latency data transmission," *J. Lightwave Technol.* **34**, 104–113 (2016).
5. J. L. Archambault, R. J. Black, S. Lacroix, and J. Bures, "Loss calculations for antiresonant wave-guides," *J. Lightwave Technol.* **11**, 416–423 (1993).
6. F. Benabid, J. C. Knight, G. Antonopoulos, and P. St.J. Russell, "Stimulated Raman scattering in hydrogen-filled hollow-core photonic crystal fiber," *Science* **298**, 399–402 (2002).
7. A. D. Pryamikov, A. S. Biriukov, A. F. Kosolapov, V. G. Plotnichenko, S. L. Semjonov, and E. M. Dianov, "Demonstration of a waveguide regime for a silica hollow-core microstructured optical fiber with a negative curvature of the core boundary in the spectral region $>3.5 \mu\text{m}$," *Opt. Express* **19**, 1441–1448 (2011).
8. P. Uebel, M. C. Gunendi, M. H. Frosz, G. Ahmed, N. N. Edavalath, J. M. Menard, and P. St.J. Russell, "Broadband robustly single-mode hollow-core PCF by resonant filtering of higher-order modes," *Opt. Lett.* **41**, 1961–1964 (2016).
9. F. Yu, W. J. Wadsworth, and J. C. Knight, "Low loss silica hollow core fibers for 3–4 μm spectral region," *Opt. Express* **20**, 11153–11158 (2012).
10. W. Belardi and J. C. Knight, "Hollow antiresonant fibers with low bending loss," *Opt. Express* **22**, 10091–10096 (2014).
11. V. Setti, L. Vincetti, and A. Argyros, "Flexible tube lattice fibers for terahertz applications," *Opt. Express* **21**, 3388–3399 (2013).
12. G. K. Alagashev, A. D. Pryamikov, A. F. Kosolapov, A. N. Kolyadin, A. Y. Lukovkin, and A. S. Biriukov, "Impact of geometrical parameters on the optical properties of negative curvature hollow-core fibers," *Laser Phys.* **25**, 055101 (2015).
13. C. L. Wei, C. R. Menyuk, and J. Hu, "Bending-induced mode non-degeneracy and coupling in chalcogenide negative curvature fibers," *Opt. Express* **24**, 2228–2239 (2016).
14. S.-F. Gao, Y.-Y. Wang, X.-L. Liu, W. Ding, and P. Wang, "Bending loss characterization in nodeless hollow-core anti-resonant fiber," *Opt. Express* **24**, 14801–14811 (2016).
15. M. Michieletto, J. K. Lyngsø, C. Jakobsen, J. Lægsgaard, O. Bang, and T. T. Alkeskjold, "Hollow-core fibers for high power pulse delivery," *Opt. Express* **24**, 7103–7119 (2016).
16. A. W. Snyder and J. D. Love, *Optical Waveguide Theory, Science Paperbacks* (Chapman and Hall, 1983), p. 734.
17. J. D. Love and C. Durniak, "Bend loss, tapering, and cladding-mode coupling in single-mode fibers," *IEEE Photon. Technol. Lett.* **19**, 1257–1259 (2007).
18. E. A. J. Marcatili and R. A. Schmeltzer, "Hollow metallic and dielectric waveguides for long distance optical transmission and lasers," *Bell Syst. Tech. J.* **43**, 1783–1809 (1964).
19. M. Heiblum and J. H. Harris, "Analysis of curved optical waveguides by conformal transformation," *IEEE J. Quantum Electron.* **11**, 75–83 (1975).
20. T. A. Birks, J. C. Knight, and P. St.J. Russell, "Endlessly single-mode photonic crystal fiber," *Opt. Lett.* **22**, 961–963 (1997).
21. J. Pomplun, L. Zschiedrich, R. Klose, F. Schmidt, and S. Burger, "Finite element simulation of radiation losses in photonic crystal fibers," *Phys. Status Solidi A* **204**, 3822–3837 (2007).
22. F. Benabid and P. J. Roberts, "Linear and nonlinear optical properties of hollow core photonic crystal fiber," *J. Mod. Opt.* **58**, 87–124 (2011).